NANO · MICRO small
www.small-journal.com

Targeting the Skin: The Study of a Bottlebrush Polymer-Antisense Oligonucleotide Conjugate in a Psoriasis Mouse Model

*Yang Fang, Jiansong Cai, Feng Fei, Tongtong Zhong, Mengqi Ren, Dali Wang, Yao Li, and Ke Zhang**

The investigation of gene regulation therapeutics for the treatment of skin-related diseases is rarely explored in part due to inefficient systemic delivery. In this study, a bottlebrush polymer-antisense oligonucleotide (ASO) conjugate, termed pacDNA, designed to target IL-17 receptor A (IL-17RA), which is involved in psoriasis pathogenesis is presented. Systemic administration of pacDNA led to its accumulation in epidermis, dermis, and hypodermis of mouse skin, reduced IL-17RA gene expression in skin, and significantly reversed the development of imiquimod (IMQ)-induced psoriasis in a mouse model. These findings highlight the potential of the pacDNA as a promising nanoconstruct for systemic oligonucleotide delivery to the skin and for treating psoriasis and other skin-related disorders through systemic administration.

1. Introduction

To date, the development of oligonucleotides therapeutics has been concentrated on a limited set of organs and tissues including the liver, skeletal muscle, and the central nervous system. While the skin is the largest vascularized organ of the body, the distribution and retention of intravenously (i.v.) injected oligonucleotide formulations in the skin is not as well studied.[1] The lack of interest in the skin may be in part due to the much lower content of blood-circulating oligonucleotides absorbed in the skin compared to the kidney, liver, and spleen, as suggested by current studies.[2]

Recently, our group has developed a form of PEGylated oligonucleotide, termed pacDNA (polymer-assisted compaction of DNA), which consists typically of 1–3 ASO strands covalently attached to the backbone of bottlebrush polymer with ≈30 polyethylene glycol(PEG) side chains.[3] Such a structure, interestingly, does not generate anti-PEG antibodies after repeated i.v. dosing, while linear PEG under an identical dosing regimen would lead to significant adaptive immunity. In addition, pacDNA exhibits a favorable safety profile.[4] Being sufficiently large to evade renal clearance, the pacDNA exhibits markedly prolonged blood circulation times with two orders of magnitude greater plasma area-under-the-curve compared to free oligonucleotides.[5] We hypothesize that the long plasma pharmacokinetics (PK) combined with the rich terminal networks of blood supply capillaries in the skin will provide the bottlebrush polymer a kinetic advantage to be absorbed by skin cells, which makes the pacDNA a promising vehicle to address skin diseases using the oligonucleotide modality.

Here, for a proof-of-concept study, we have investigated pacDNA in a psoriasis-like mouse model. Psoriasis is an immune-mediated chronic inflammatory skin disease characterized by keratinocytes hyperproliferation, parakeratosis, and immune cells infiltration (including monocytes, *T*-cells, and neutrophils).[6] Recent studies demonstrate that psoriasis pathogenesis strongly depends on the IL-23/IL-17 axis; the cytokines such as IL-17A and IL-17F which are secreted by T-helper 17 (Th17) cells play a critical role in the development of the disease.[7] Therefore, many biological agents targeting Th17 cells, their related cytokines, and receptors such as IL-17 receptor A (IL-17RA) have been developed to treat psoriasis.[8] For example, both systemic administration of monoclonal antibodies blocking IL-17A (ixekizumab[9] and secukinumab)[10] and IL-17RA (brodalumab)[11] have shown high efficacy for the

Y. Fang, J. Cai, F. Fei, M. Ren, D. Wang
Department of Chemistry and Chemical Biology
Northeastern University
Boston, MA 02115, USA
T. Zhong
Bouvé College of Health Sciences
Northeastern University
Boston, MA 02115, USA
Y. Li
Department of Bioengineering
Northeastern University
Boston, MA 02115, USA
K. Zhang
Departments of Chemistry and Chemical Biology
Chemical Engineering
and Bioengineering
Northeastern University
Boston, MA 02115, USA
E-mail: k.zhang@northeastern.edu

The ORCID identification number(s) for the author(s) of this article can be found under https://doi.org/10.1002/smll.202403949

DOI: 10.1002/smll.202403949

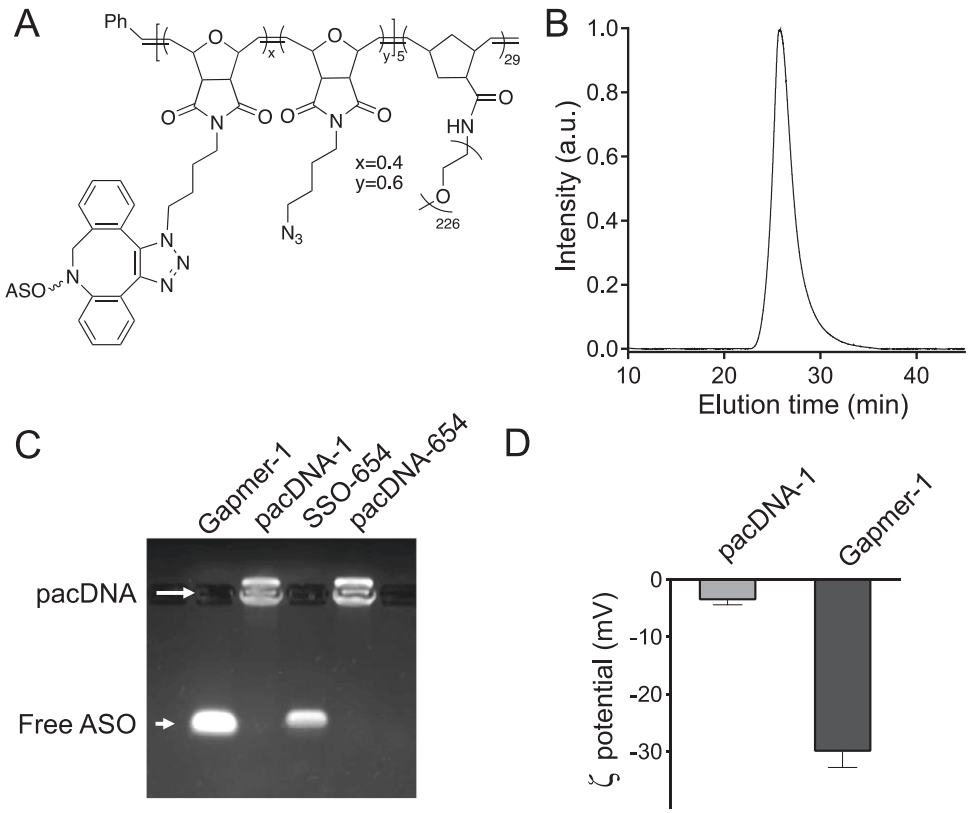

Figure 1. Physiochemical characterization of pacDNA. A) Chemical structure of pacDNA. B) Aqueous gel permeation chromatogram of pacDNA-1. C) Agarose gel electrophoresis (2%) free ASO and pacDNA counterparts. D) Zeta potential measurements of gapmer-1 and pacDNA-1 in Nanopure water.

treatment of moderate-to-severe psoriasis cases.[12] Nucleic acid-based skin therapeutic candidates, including ASOs, microRNAs, and small interfering RNAs (siRNAs), have been envisioned but are largely focused on topical transdermal delivery, which suffer from poor skin penetration, short half-lives, and limited target engagement.[13] Systemic application of nucleic acid-based therapeutics to treat skin pathologies can in principle alleviate these difficulties but poses a significant delivery challenge.[14]

2. Results and Discussion

2.1. Preparation and Characterization of pacDNA

The synthesis of pacDNA followed protocols as described in prior literature (Scheme S1, Supporting Information).[15] Table S1 (Supporting Information) presents the ASO sequences used in this study. Briefly, to synthesize the diblock bottlebrush polymer, a sequential ring-opening metathesis polymerization (ROMP) reaction is employed using two monomers: 7-oxanorbornenyl bromide (N-Br)[16] and norbornenyl-modified PEG (N-PEG) at a ratio of 5:35. The reaction yields a diblock architecture (pNBr_5-*b*-p$NPEG_{29}$, yield: 93%, M_n: 290 kDa, PDI: 1.20), which was characterized by *N,N*-dimethylformamide gel permeation chromatography (DMF-GPC)(Figure S1, Supporting Information). Next, azide substitution of bromides and subsequent coupling with dibenzocyclooctyne (DBCO)-modified ASO strands are carried out. After the removal of unconjugated ASOs by aqueous GPC, purified pacDNA conjugates with an average of 1.9 ASO strands per polymer are obtained (**Figure 1**). Agarose gel electrophoresis shows significantly decreased electrophoretic mobility compared with free ASO following the conjugation reaction. Dynamic light scattering (DLS) revealed the presence of nanoparticles with a Z-average hydrodynamic diameter of 30 ± 2 nm. Furthermore, and ζ potential measurements indicated that pacDNA-1, which contains a gapmer ASO (gapmer-1, Table S1, Supporting Information), exhibited a slight negative charge of ≈−4 to −2 mV, which represents a significant reduction in negative surface charge compared to the free gapmer of ≈−30 mV.

To assess the biodistribution of bottlebrush polymer, cyanine5 (Cy5)-labeled bottlebrush polymer was injected into the tail vein of C57BL/6 mice. Fluorescence imaging of dissected major internal organs and the skin 24 h after injection was carried out, showing pronounced uptake into the mouse skin (**Figure 2A**). In fact, the skin exhibited the highest uptake level among all organs tested, as determined by average radiant efficiency (Figure S2, Supporting Information) or by fluorescence intensity of tissue homogenates (Figure 2B; Figure S3, Supporting Information). The latter allows us to determine the skin uptake as % injected dose/gram (%ID/g) of skin tissue. The bottlebrush polymer exhibits 11.0%ID/g in the skin. For comparison, 2′-*O*-(2-methoxyethyl)-modified (OMe-modified) phosphorothioate (PS) oligonucleotide shows skin uptake of 0.17%ID/g,[17] while co-carriers considered of clinical relevance for oligonucleotide delivery such as cationic liposomes have the skin uptake at

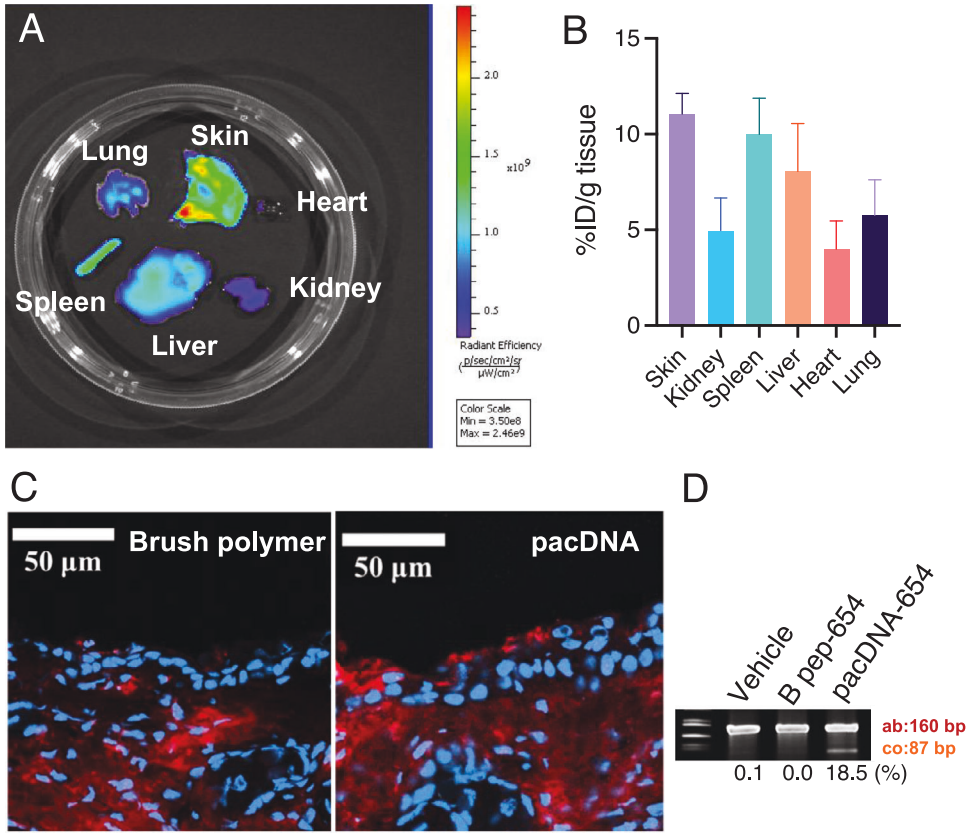

Figure 2. Biodistribution and target engagement in mice. A) Ex vivo imaging of mouse dorsal skin and other major organs 24 h post tail vein injection of Cy5-bottlebrush polymer and B) Quantitative biodistribution determined using tissue homogenate. C) Representative fluorescence micrograph of mouse dorsal skin cryosection (OCT-embedded) 24 h after injection (Cy5 label resides on ASO component). Cell nuclei are stained with Hoechst 33342. D) EGFP transcript isolated from skin tissue of EGFP-654 mice after treatment as determined by RT-PCR. Bands shown as "Ab" (160 bp) and "Co" (87 bp) represent aberrantly spliced and correctly spliced EGFP mRNA, respectively.

≈1.81%ID/g.[18] Of note, the comparison is approximate as dosing, dosing frequency, and species vary across different studies. We attribute this effect to the extended plasma PK and the rich vasculature of skin tissues. The polymer is able to impart its skin distribution to conjugated oligonucleotides, as pacDNA-1's skin distribution is significantly more evident compared with the free gapmer-1 as determined by *ex vivo* imaging (Figure S4, Supporting Information).

2.2. Skin Distribution

Next, we performed an immunohistological study regarding the sub-organ localization of brush polymer within the skin. 24 h after i.v. injection of Cy5-labeled bottlebrush polymer, the dorsal skin tissues of C57BL/6 mice were harvested, and fluorescence microscopy of cryosectioned skin reveals that the bottlebrush polymer is present across the epidermis, dermis, and hypodermis (Figure 2C; Figure S5, Supporting Information). Immunofluorescence staining shows that the polymer is taken up by skin-resident macrophages ($F4/80^+$),[19] dendritic cells ($CD11c^+$),[19] fibroblasts (vimentin),[20] and adipose cells (perilipin-1 and bright field)[21] (Figure S6, Supporting Information). In addition, fluorescence signals were observed in pericellular space of the dermis, which may be due to diffusion and exocytotic activities.[1b] When gapmer-1 was conjugated to the bottlebrush polymer (i.e., the pacDNA), a similar signal intensities and distribution pattern was observed compared to the bottlebrush polymer alone (Figure 2C; Figure S7, Supporting Information).

2.3. Splicing Switching in the Skin

With the promising skin distribution, we next evaluated the antisense activity of i.v. injected pacDNA in the skin utilizing the EGFP-654 transgenic mice, which express a modified enhanced green fluorescence protein (EGFP) pre-mRNA containing an aberrantly spliced human β-globin intron (IVS2-654).[15,22] When a splice-switching oligonucleotide (SSO) binds to the aberrant 5′ splicing site (Figure S8, Supporting Information), correct splicing can be restored resulting in the subsequent production of functional EGFP mRNA.[23] EGFP-654 mice were administrated with pacDNA bearing a full locked nucleic acid (LNA) SSO targeting the aberrant splice site (pacDNA-654, 1.0 µmol kg^{-1}, SSO basis), vehicle (phosphate buffered saline, PBS), or arginine-rich cell-penetrating peptide conjugated (B pep-654, 1.0 µmol kg^{-1}, SSO basis)[24] once daily for consecutive four days (Figure S9, Supporting Information). Animals were euthanized one week

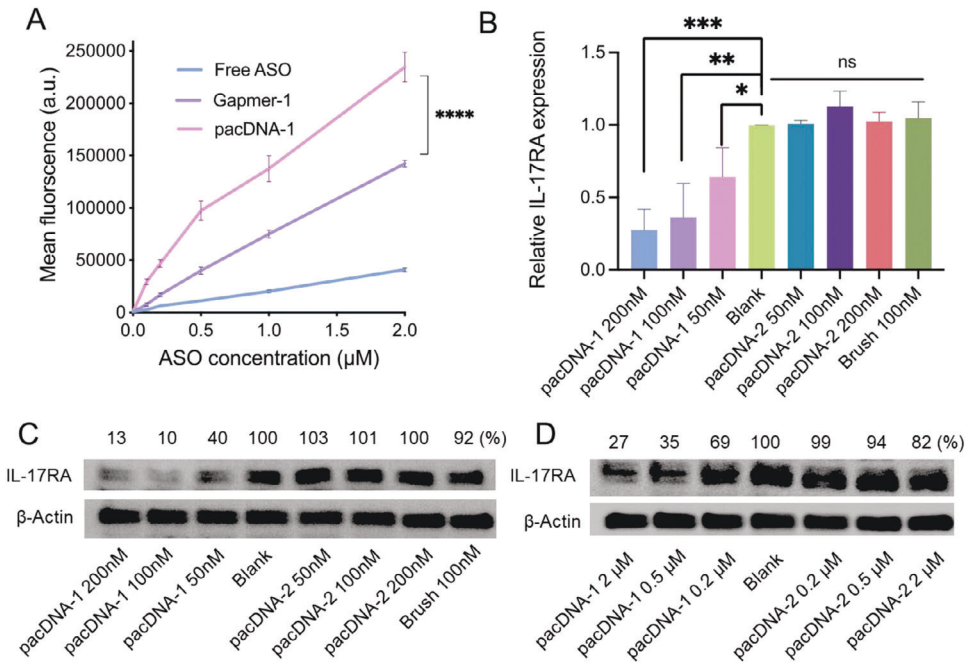

Figure 3. In vitro uptake and IL-17RA silencing. A) Cellular uptake of Cy5-labeled pacDNA, unmodified DNA ASO, and gapmer-1 by NIH/3T3 cells (0.1 to 2 μM ASO, 4 h) as determined by flow cytometry. B) Dose-dependent reduction of IL-17RA in RAW 264.7 cells by pacDNA-1 (72 h treatment). C,D) Western blot analysis of IL-17RA protein levels in RAW 264.7 and NIH/3T3 cells after treatment with pacDNA-1, pacDNA-2, or bottlebrush polymer (72 h). $^{*}p < 0.05$, $^{**}p < 0.01$, $^{***}p < 0.001$, $^{****}p < 0.0001$ (two-tailed test).

after the last administration, and the RNA was extracted from skin tissues for reverse transcriptase-PCR (RT-PCR) analysis. pacDNA-treated mice exhibited partially restored splicing in the skin (≈20%), indicating that skin-accumulated pacDNA can enter cells and engage with intracellular targets, while both controls showed no detectable EGFP mRNA (Figure 2D). This result also suggests that the pacDNA can be designed to address targets within the cell nucleus, despite the fact the pacDNA is a non-cleavable conjugate with a molecular weight ≈300 kDa.

2.4. Psoriasis Mouse Model

We next set out to explore the activity of pacDNA using psoriasis as a model disease. We first synthesized pacDNA targeting IL-17RA (pacDNA-1) and investigated its cellular uptake using NIH/3T3 mouse fibroblasts. Cells were treated with Cy5-labeled pacDNA-1 or two naked ASOs: a gapmer DNA with flanking PS and 2′ OMe modifications (Table S1, Supporting Information) and an unmodified DNA ASO. Flow cytometry showed that pacDNA-1 bearing the gapmer sequence exhibited higher cell uptake, roughly approximately ten-fold greater than unmodified ASO and approximately four-fold higher than the gapmer at 0.1 μM (**Figure** 3A; Figure S10, Supporting Information). To measure antisense activity, IL-17RA protein expression levels from NIH/3T3 and RAW 264.7 cells were measured by western blot after cells were treated with pacDNA-1, scrambled pacDNA control (pacDNA-2), and free bottlebrush polymer (Figure 3 B,C,D). It was observed that pacDNA-1 reduced IL-17RA expression in a dosage-dependent manner, with a maximum reduction level of ≈70–90%, while negative control samples exhibited no detectable target depletion.

To test the in vivo efficacy of pacDNA-1 to suppress the development of the psoriasis-like phenotype after i.v. administration, an IMQ-induced mouse model of psoriasis based upon C57BL/6 mice was used. Topical application of IMQ to the skin induces psoriasis-like dermatitis in mice with many characteristics of human psoriasis, including the formation of microabscesses, acanthosis, parakeratosis, hyperkeratosis, hyperplasia, erythema, and scaling.[25] IMQ cream (5%) was topically applied to shaved mouse dorsal skin daily for six consecutive days to induce psoriasis-like skin lesions. pacDNA-1, pacDNA-2, or vehicle (PBS) was injected through mouse tail vein (20 nmol ASO per animal) on days 1, 3, and 5 (Figure S11, Supporting Information). To examine the severity of the phenotype, the Psoriasis Area and Severity Index (PASI) was used, which is formulated by evaluating the degree of erythema (redness), induration (thickness), and desquamation (scaling) of the affected skin area.

The development of psoriasis-like dermatitis from pacDNA-1-treated group was evidently suppressed when compared to pacDNA-2 and vehicle groups (**Figure** 4A). Mice in the pacDNA-1-treated group showed a marked decrease in overall PASI score (60%, Figure 4B) with redness (69%, Figure 4C), thickness (52%, Figure 4D), and scaling (61%, Figure 4E) separately compared to vehicle-treated group, indicating the efficacy of pacDNA-1 in alleviating the psoriasis-like changes. In addition to the PASI scoring, the degree of skin erythema (i.e., redness of hemoglobin)[26] was also quantitatively evaluated by a tristimulus colorimeter and shown as a^* of CIE$L^*a^*b^*$ (CIELAB) color space, which has been frequently used as an indicator of skin erythema.[27] The a^*

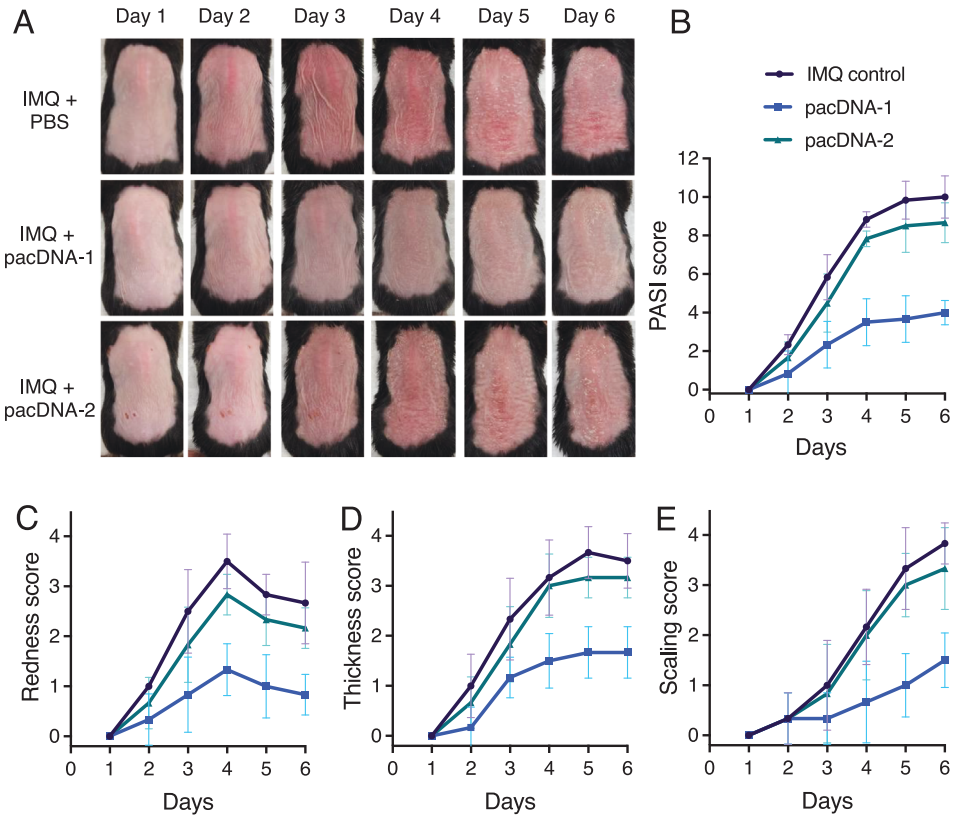

Figure 4. In vivo phenotypic response. A) Representative images of mouse dorsal skin of each group. B) Disease progression as indicated by PASI score (cumulative score of thickness plus erythema plus scaling, score: 0–12) as assessed by six blinded reviewers. C–E) Individual scoring redness, thickness, and scaling on a scale from 0–4.

values of mouse dorsal skin, which were recorded daily (Figure S12, Supporting Information), also show a pronounced reduction in redness for the pacDNA-1-treated mice compared to negative control groups. Remarkably, pacDNA-1 was dosed at 5 mg kg^{-1} (ASO mass only), which is significantly lower than what is typical of this drug modality (on the order of tens to >100 mg kg^{-1}). The notable bioactivity at such low dosages is attributed to the evasion of renal clearance and greatly increased accumulation in the site of pathology.

To further investigate the effect of pacDNA-1 on the tissue, cell, and biochemical levels, mouse dorsal skin was harvested on day 7 and evaluated for histological features and IL-17RA expression. Comparing with the vehicle and pacDNA-2-treated groups, the extent of these psoriatic histological characteristics of skin from the pacDNA-1-treated group were marked reduced (**Figure** 5A). In particular, epidermal thickness decreased by 53% compared to the PBS control group (Figure 5C). In addition, the number of Ki-67-positive cells at basal layers was decreased by 78% with the treatment of pacDNA-1 (Figure 5B,D). Overexpression of Ki-67 protein is associated with abnormal keratinocyte proliferation, a characteristic of psoriasis.[28] Finally, the expression of IL-17RA was directly determined by western blot using homogenized skin cells and immunohistochemical staining (Figure S13, Supporting Information). Band densitometry analysis of western blot bands shows that skin tissue from pacDNA-1-treated group express 69% less IL-17RA protein compared to the PBS control (Figure 5E). Down-regulation of IL-17RA is associated with significantly decreased the transcript level of several psoriasis-related markers including Pi3 (46% reduction, Figure S14A, Supporting Information), TNFα (61% reduction, Figure S14B, Supporting Information), and IL17C (57% reduction, Figure S14C, Supporting Information) compared to the pacDNA-2 treatment group.

3. Conclusion

In summary, we have demonstrated that pacDNA is a highly effective agent to realize skin delivery of oligonucleotide therapeutics with systemic administration. The conjugate preferentially accumulates in the skin, distributes across all skin layers, and gains access to skin cells and skin-resident immune cells. The elevated skin uptake and retention allow a markedly lower dose of oligonucleotide to be used compared to conventional formulations to achieve a comparable phenotypic response. Using an IMQ-induced psoriasis mouse model, the pacDNA effectively engages with the target, reduces the severity of the symptoms, and reverses the development of psoriasis phenotypically, translationally, and histologically. This study opens the door to developing new therapies for a range of skin disorders with a genetic basis that are previously recalcitrant to treatment.

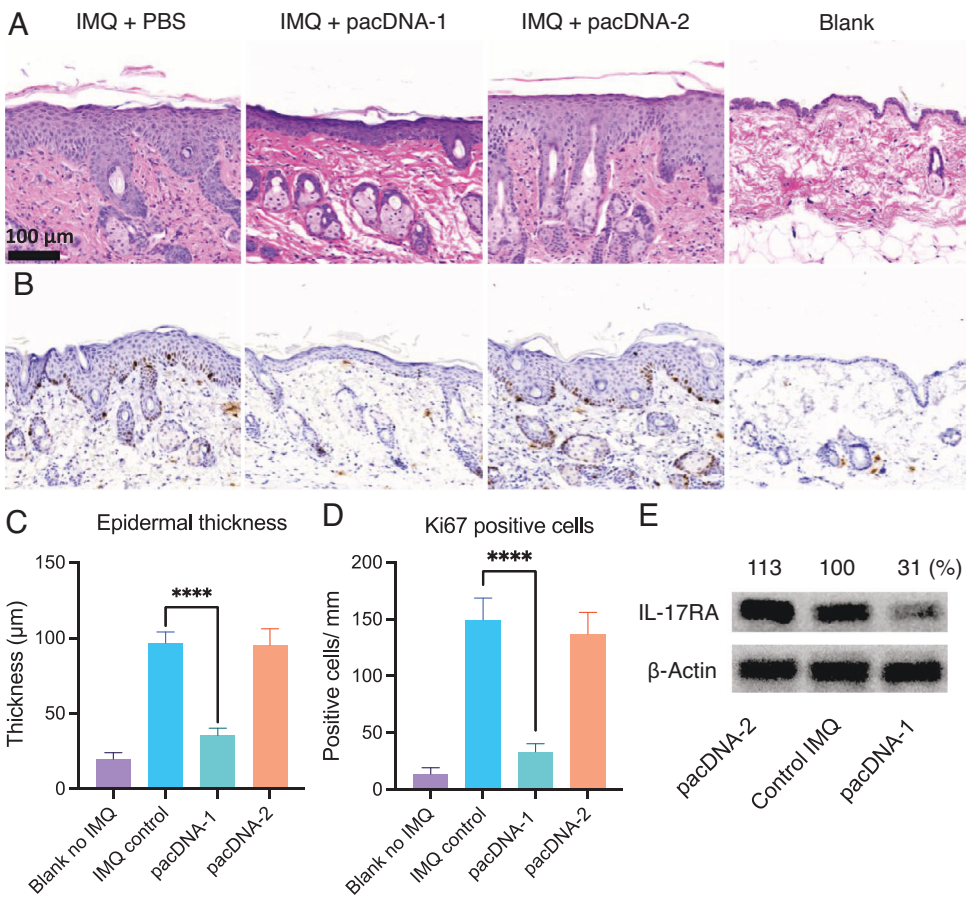

Figure 5. Biochemical and histological analysis. A) Representative hematoxylin and eosin (H&E) and B) Ki67 immunohistochemical staining of mouse dorsal skin collected on day 7. C) Average epidermal thickness measured from multiple H&E-stained images. D) The number of epidermal Ki67-positive cells of each group counted in five areas. $^{****}p < 0.0001$ (two-tailed test). E) Expression levels of IL-17RA in the dorsal skin of IMQ-induced mouse with injection of pacDNA-1, pacDNA-2, or vehicle only as determined by western blot.

Supporting Information

Supporting Information is available from the Wiley Online Library or from the author.

Received: May 17, 2024
Revised: July 12, 2024
Published online:

Acknowledgements

The authors thank Dr. Guoxin Rong from the Institute for Chemical Imaging of Living System at Northeastern University for assistance with confocal microscopy, and Dr. Mansoor M. Amiji for IVIS imaging.

Conflict of Interest

K.Z., Y.F., and F.F. hold financial interest in pacDNA Inc., a company commercializing the pacDNA technology.

Data Availability Statement

The data that support the findings of this study are available in the supplementary material of this article.

Keywords

bottlebrush polymer, oligonucleotide, psoriasis, skin, splicing correction

[1] a) E. Sutterby, P. Thurgood, S. Baratchi, K. Khoshmanesh, E. Pirogova, *Small* **2020**, *16*, 2002515; b) E. A. Sykes, Q. Dai, K. M. Tsoi, D. M. Hwang, W. C. Chan, *Nat. Commun.* **2014**, *5*, 3796.

[2] a) H. Wang, W. Sheng, *Nanoscale Res. Lett* **2017**, *12*, 365; b) C. Alric, I. Miladi, D. Kryza, J. Taleb, F. Lux, R. Bazzi, C. Billotey, M. Janier, P. Perriat, S. Roux, O. Tillement, *Nanoscale* **2013**, *5*, 5930.

[3] a) F. Jia, X. Lu, D. Wang, X. Cao, X. Tan, H. Lu, K. Zhang, *J. Am. Chem. Soc.* **2017**, *139*, 10605; b) X. Lu, T.-H. Tran, F. Jia, X. Tan, S. Davis, S. Krishnan, M. M. Amiji, K. Zhang, *J. Am. Chem. Soc.* **2015**, *137*, 12466; c) Y. Wang, D. Wang, F. Jia, A. Miller, X. Tan, P. Chen, L. Zhang, H. Lu, Y. Fang, X. Kang, J. Cai, M. Ren, K. Zhang, *ACS Appl. Mater. Interfaces* **2020**, *12*, 45830; d) F. Jia, P. Chen, D. Wang, Y. Sun, M. Ren, Y. Wang, X. Cao, L. Zhang, Y. Fang, X. Tan, H. Lu, J. Cai, X. Lu, K. Zhang, *ACS Appl. Mater. Interfaces* **2021**, *13*, 42533; e) Y. Fang, K. Zhang, *Encyclopedia of Nanomaterials*, 1st Ed., (Eds: Y. Yin, Y. Lu, Y. Xia), Elsevier, **2023**, pp. 574–589, https://doi.org/10.1016/B978-0-12-822425-0.00024-5; f) L. Zhang, Y. Wang, P. Chen, D. Wang, T. Sun, Z. Zhang, R. Wang, X. Kang, Y. Fang, H. Lu, J. Cai, M. Ren, S. S. Dong, K. Zhang, *RSC Chem Biol* **2023**, *4*, 138.

[4] Y. Wang, D. Wang, J. Lin, Z. Lyu, P. Chen, T. Sun, C. Xue, M. Mojtabavi, A. Vedadghavami, Z. Zhang, R. Wang, L. Zhang, C. Park, G. S. Heo, Y. Liu, S. S. Dong, K. Zhang, *Angew. Chem., Int. Ed.* **2022**, *61*, 202204576.
[5] D. Wang, J. Lin, F. Jia, X. Tan, Y. Wang, X. Sun, X. Cao, F. Che, H. Lu, X. Gao, J. C. Shimkonis, Z. Nyoni, X. Lu, K. Zhang, *Sci. Adv.* *5*, eaav9322.
[6] a) S. K. Ippagunta, R. Gangwar, D. Finkelstein, P. Vogel, S. Pelletier, S. Gingras, V. Redecke, H. Häcker, *Proc. Natl. Acad. Sci. USA* **2016**, *113*, E6162; b) K. T. Lewandowski, R. Thiede, N. Guido, W. L. Daniel, R. Kang, M. I. Guerrero-Zayas, M. A. Seeger, X. Q. Wang, D. A. Giljohann, A. S. Paller, *J. Invest. Dermatol.* **2017**, *137*, 2027.
[7] B. Li, L. Huang, P. Lv, X. Li, G. Liu, Y. Chen, Z. Wang, X. Qian, Y. Shen, Y. Li, W. Fang, *Immunol. Res.* **2020**, *68*, 296.
[8] A. Blauvelt, *J. Invest. Dermatol* **2008**, *128*, 1064.
[9] E. Toussirot, *Expert Opin. Biol. Ther.* **2018**, *18*, 101.
[10] K. Reich, A. Blauvelt, A. Armstrong, R. G. Langley, A. de Vera, F. Kolbinger, S. Spindeldreher, M. Ren, G. Bruin, *J. Eur. Acad. Dermatol. Venereol.* **2019**, *33*, 1733.
[11] L. Puig, *Drugs Today (Barc)* **2017**, *53*, 283.
[12] C. Jeon, S. Sekhon, D. Yan, L. Afifi, M. Nakamura, T. Bhutani, *Hum. Vaccines Immunother.* **2017**, *13*, 2247.
[13] a) V. K. Rapalli, T. Waghule, S. Gorantla, S. K. Dubey, R. N. Saha, G. Singhvi, *Drug Discov.* **2020**, *25*, 2212; b) H. Liu, R. S. Kang, K. Bagnowski, J. M. Yu, S. Radecki, W. L. Daniel, B. R. Anderson, S. Nallagatla, A. Schook, R. Agarwal, D. A. Giljohann, A. S. Paller, *J. Invest. Dermatol.* **2020**, *140*, 435; c) P. Sharma, A. Kumar, T. Agarwal, A. D. Dey, F. D. Moghaddam, I. Rahimmanesh, M. Ghovvati, S. Yousefiasl, A. Borzacchiello, A. Mohammadi, V. R. Yella, O. Moradi, E. Sharifi, *Int. J. Biol. Macromol.* **2022**, *220*, 920; d) M. Zakrewsky, S. Kumar, S. Mitragotri, *J. Control Release* **2015**, *219*, 445.
[14] a) B. Gurav, G. Srinivasan, *Curr. Sci.* **2017**, *112*, 490; b) Y. Weng, Q. Huang, C. Li, Y. Yang, X. Wang, J. Yu, Y. Huang, X.-J. Liang, *Mol. Ther. Nucleic Acids* **2020**, *19*, 581.
[15] Y. Fang, J. Cai, M. Ren, T. Zhong, D. Wang, K. Zhang, *ACS Nano* **2024**, *18*, 592.
[16] a) Y. Fang, X. Lu, D. Wang, J. Cai, Y. Wang, P. Chen, M. Ren, H. Lu, J. Union, L. Zhang, Y. Sun, F. Jia, X. Kang, X. Tan, K. Zhang, *J. Am. Chem. Soc.* **2021**, *143*, 1296; b) P. Chen, D. Wang, Y. Wang, L. Zhang, Q. Wang, L. Liu, J. Li, X. Sun, M. Ren, R. Wang, Y. Fang, J. J. Zhao, K. Zhang, *Nano Lett.* **2022**, *22*, 4058.
[17] a) M. K. Bijsterbosch, E. T. Rump, R. L. A. D. Vrueh, R. Dorland, R. van Veghel, K. L. Tivel, E. A. L. Biessen, T. J. C. van Berkel, M. Manoharan, *Nucleic Acids Res.* **2000**, *28*, 2717; b) R. S. Geary, R. Z. Yu, T. Watanabe, S. P. Henry, G. E. Hardee, A. Chappell, J. Matson, H. Sasmor, L. Cummins, A. A. Levin, *Drug Metab. Dispos.* **2003**, *31*, 1419.
[18] D. C. Litzinger, J. M. Brown, I. Wala, S. A. Kaufman, G. Y. han, C. L. Farrell, D. Collins, *Biochim. Biophys. Acta Biomembr.* **1996**, *1281*, 139.
[19] M. Dupasquier, P. Stoitzner, A. v. Oudenaren, N. Romani, P. J. M. Leenen, *J. Invest. Dermatol.* **2004**, *123*, 876.
[20] a) S.-S. Kim, S.-J. Gwak, C. Y. Choi, B.-S. Kim, *J. Biomed. Mater. Res* **2005**, *75B*, 369; b) F. Bernerd, D. Asselineau, *Cell Death Differ.* **1998**, *5*, 792; c) W. Mah, G. Jiang, D. Olver, C. Gallant-Behm, C. Wiebe, D. A. Hart, L. Koivisto, H. Larjava, L. Häkkinen, *Am. J. Clin. Pathol.* **2017**, *187*, 1717.
[21] C. Miggitsch, A. Meryk, E. Naismith, L. Pangrazzi, A. Ejaz, B. Jenewein, S. Wagner, F. Nägele, G. Fenkart, K. Trieb, W. Zwerschke, B. Grubeck-Loebenstein, *EBioMedicine* **2019**, *46*, 387.
[22] P. Sazani, F. Gemignani, S.-H. Kang, M. A. Maier, M. Manoharan, M. Persmark, D. Bortner, R. Kole, *Nat. Biotechnol* **2002**, *20*, 1228.
[23] J. Roberts, E. Palma, P. Sazani, H. Ørum, M. Cho, R. Kole, *Mol. Ther.* **2006**, *14*, 471.
[24] N. B. Lu-Nguyen, S. A. Jarmin, A. F. Saleh, L. Popplewell, M. J. Gait, G. Dickson, *Mol. Ther.* **2015**, *23*, 1341.
[25] a) L. van der Fits, S. Mourits, J. S. Voerman, M. Kant, L. Boon, J. D. Laman, F. Cornelissen, A.-M. Mus, E. Florencia, E. P. Prens, E. Lubberts, *J. Immunol.* **2009**, *182*, 5836; b) C. E. Griffiths, J. N. Barker, *Lancet* **2007**, *370*, 263; c) M. W. Greaves, G. D. Weinstein, *N. Engl. J. Med.* **1995**, *332*, 581.
[26] M. Baquié, B. Kasraee, *Skin Res Technol* **2014**, *20*, 218.
[27] a) J. C. Seitz, C. G. Whitmore, *Dermatology (Basel)* **1988**, *177*, 70; b) M. H. A. Fadzil, D. Ihtatho, A. Mohd Affandi, S. H. Hussein, *J Med Eng Technol* **2009**, *33*, 516.
[28] L. Li, H.-y. Zhang, X.-q. Zhong, Y. Lu, J. Wei, L. Li, H. Chen, C. Lu, L. Han, *Life Sci.* **2020**, *243*, 117231.